Rotational spectra and structures of small clusters containing the HCN dimer: (HCN)₂–Ar, a T-shaped trimer

R. S. Ruoff, T. I. Emilsson, T. D. Klots, C. Chuang, and H. S. Gutowsky
Noyes Chemical Laboratory, University of Illinois, Urbana, Illinois 61801

Microwave rotational spectra have been observed for the four $^{14}N/^{15}N$ isotopic species of an $(HCN)_2$–Ar trimer with the pulsed nozzle Fourier transform method using the Flygare Mark II spectrometer. Thirteen $J \rightarrow J'$ asymmetric top transitions were measured in the 2.5 to 10 GHz region for the parent $^{14}N,^{14}N$ trimer and nine for each of the other three species. The ^{14}N nuclear quadrupole hyperfine structure was analyzed for the transitions and the interaction constants and line centers determined. The line centers were fitted to obtain ground vibronic state rotational and quartic centrifugal distortion constants. For the $^{14}N/^{14}N$ trimer these are (in MHz) for A'', B'', and C'': 2013.5993(10), 1759.2756(3), 932.3709(2); and for τ_1, τ_2, τ_{aaaa}, τ_{bbbb}, and τ_{cccc}: $-0.3017(1)$, $-0.0660(1)$, $-0.1700(9)$, $-0.013\ 71(1)$, and $-0.0088(1)$. The inertial defect is 3.7881 amu Å^2. The zero-point vibrationally averaged geometry is planar and T shaped with the structure of the linear HCN dimer remarkably unperturbed by presence of the Ar atom. The substitution $N \cdots N$ distance in the cluster is 4.453 Å compared with 4.461 Å in the free dimer. The argon is attracted by the π electrons of the two $-C \equiv N$ groups, being equidistant from them. The $Ar \cdots N(1)$ and $Ar \cdots N(2)$ distances are 3.671 and 4.316 Å, respectively.

INTRODUCTION

HCN is known to form a strong, linear, hydrogen-bonded dimer $(HCN)_2$ with a Lennard-Jones well depth ϵ of 1540 cm^{-1}.[1,2] In turn, the dimer serves as the major subunit in a variety of linear or quasilinear trimers such as HCN–$(HCN)_2$,[3] N_2–$(HCN)_2$, or $(HCN)_2$–HCl,[4] in which the third molecular element is also hydrogen bonded. The geometries of these trimers, X–$(HCN)_2$ or $(HCN)_2$–Y, are predictable as a composite of the corresponding two dimers, X–HCN or HCN–Y and HCN–HCN.

Based on this simple viewpoint, we undertook a search for a linear Ar–$(HCN)_2$ trimer, given that both Ar–HCN[5] and HCN–HCN[2] have linear geometries and using their dimensions to determine the search window. However, the search was not successful. Instead, the trimer which is the subject of this paper was found later on by accident. The first indication of it was a set of 11 quite strong lines, to which 5 weaker ones were added later, all centered at 4555.75 MHz and extending over ~ 4 MHz (Fig. 1). Their appearance is reminiscent of the $J = 1 \rightarrow 2$ and $2 \rightarrow 3$ transitions of the $(HCN)_2$ dimer,[1] indicating a small cluster containing it as a subunit. A more detailed study was undertaken which confirmed this possibility. It included analysis of the hyperfine structure (hfs), a search for related transitions and study of the species formed by isotopic substitution of ^{15}N for ^{14}N. The analysis was expedited by a methodology for determining Ray's asymmetry parameter $\kappa = (2B-A-C)/(A-C)$, from the hfs, a procedure which should prove useful for other small, asymmetric clusters.

The details of the study are presented below. The cluster is found to be T shaped with a remarkably unperturbed linear $(HCN)_2$ as the top of the T and an argon atom as the bottom of its stem. The argon is almost directly below the H

in the hydrogen bond, virtually equidistant from the center of mass (c.m.) of HCN(1) and of HCN(2). In retrospect, a cluster of this structure is not too surprising. Previous studies of HCN-containing dimers and trimers have found linear structures determined by hydrogen bonding.[1–5] However, the π electrons of the $-C \equiv N$ group can also be a locus of intermolecular attraction. This is suggested by the Ar–HCN dimer which, although linear and formed by an attraction to hydrogen, is unusually floppy with huge centrifugal distortion effects[5] apparently associated with interactions between Ar and the π electrons.

The complexity of the interaction potential between argon and HCN is underscored by current high-resolution work of our group which shows that the ^{14}N hyperfine inter-
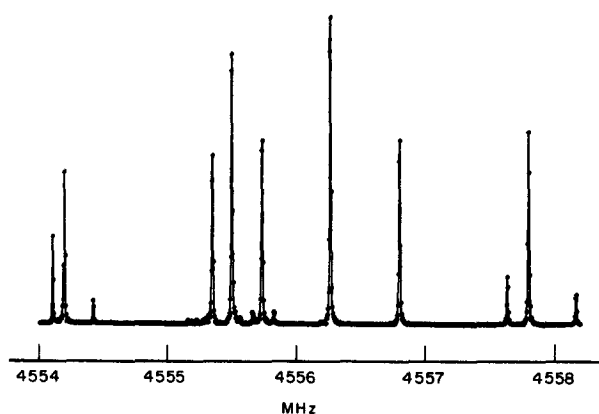

FIG. 1. Hyperfine structure centered at 4555.749 MHz observed for the $1_{11} \rightarrow 2_{12}$ transition of $(HC^{14}N)_2$–Ar. The spectrum is a composite of 12 segments joined by computer. Between 100 and 1700 FIDs were averaged for individual segments.

action in Ar–HCN is J dependent, becoming *larger* at higher J.[6] The T-shaped Ar_2–HCN trimer exhibits a similar dependence and, although possessing C_{2v} symmetry, has an enormous inertial defect of 13.5 amu Å^2.[6] These peculiarities are probably a consequence of competing interactions of the argon with the hydrogen and the π electrons of HCN. In our present study the π-electron interactions appear to dominate the attraction of the Ar by the hydrogen bonded dimer.

EXPERIMENTAL

The Mark II spectrometer used to acquire the spectra for the present study has been discussed previously.[7,8] Briefly, a pulse of argon mixed with a small percentage of HCN is introduced to an evacuated Fabry–Perot cavity through a supersonic nozzle. As it expands, it cools and small clusters form, which are subjected to a microwave pulse of adjustable duration, power, and frequency. When on resonance, the sample becomes polarized and produces a free induction decay (FID) signal in the cavity after the polarizing pulse. The signal is detected, digitized, accumulated, and Fourier transformed to provide the frequency spectrum, as in Fig. 1. In expansion, the gas mixture achieves a rotational temperature of about 5 K.

For $(HCN)_2$–Ar, the best signal to noise was obtained with a mixture of about 0.1% HCN and 20% Ar in "first-run" neon (Airco), the latter being 70% neon and 30% helium. The backing pressure was typically 2 atm. Under these conditions the S/N for the stronger hyperfine components of the $1_{11} \rightarrow 2_{12}$ transition centered at 4555.749 MHz was roughly 5:1 for a single shot (microwave pulse) and about 15:1 for the same transition of $(HC^{15}N)_2$–Ar, which has no hfs. When high resolution was required Ar was used as the carrier gas and an adjustable slit assembly[8] was employed to suppress Doppler broadening.[7] Neon and helium, being lighter, have higher velocities and cause larger linewidths when used as the carrier gas. The frequencies reported for individual lines have a standard deviation of 1 kHz or better, depending on S/N and resolution.

$HC^{15}N$ was made by adding orthophosphoric acid to $KC^{15}N$ (Cambridge Isotope Laboratories). The vacuum system was modified to recover expensive isotopes of HCN with a liquid nitrogen trap just before the mechanical pump. A test of its operation was made by putting a known volume of $HC^{14}N$ through the system. Recovery was nearly 100% demonstrating that the silicone pump oil and passage of the HCN through the diffusion pump did not degrade the sample.

The relative intensities of equivalent transitions for different isotopic species of the cluster, with allowance for differences in hfs, are noteworthy. For a 50/50 mix of $^{14}N/^{15}N$ HCN, the transitions for $(HC^{14}NHC^{15}N)$–Ar and $(HC^{15}NHC^{14}N)$–Ar had about one-tenth the signal found for pure $HC^{14}N$ rather than one-fourth as expected. However, the signal for the $^{15}N/^{15}N$ species was rather more than one-fourth. In contrast, signal intensities for isotopic variants of the HCN dimer[9] and trimer[3] were roughly as predicted from the isotopic abundances.

RESULTS AND ANALYSIS

Search, hfs, and molecular geometry

$(HCN)_2$–Ar was found by luck in an unsuccessful search for a diborane–HCN dimer using Ar as the carrier gas. A set of 11 strong lines, later augmented by 5 weak ones, was observed at about 4556 MHz, extending over 5 MHz. A composite spectrum of them is given in Fig. 1, a high-resolution view of the four low-frequency components in Fig. 2, and the measured frequencies in Table I. The spread and number of hyperfine components indicated a low J transition (probably $J = 1 \rightarrow 2$) of a small cluster containing a linear (or near linear) $(HCN)_2$ dimer, such as reported previously.[1] Inclusion of argon was established by expansion of HCN in first run neon with and without argon present. Linear Ar–$(HCN)_2$ and $(HCN)_2$–Ar were ruled out by their small B_0's, estimated to be 375 and 480 MHz, respectively, for which a transition at 4556 MHz would be $J = 5 \rightarrow 6$ or $4 \rightarrow 5$. Clusters containing more than one argon were discarded for similar reasons, leaving a nonlinear $(HCN)_2$–Ar trimer as the most likely candidate.

Confirmation of this view and further details were obtained by analyzing the hfs of the 4556 MHz transition. It was fitted by full matrix diagonalization in the coupled basis

$$I_1 + I_2 = F_1, \quad J + F_1 = F, \qquad (1)$$

treating the transition as $J = 1 \rightarrow 2$. A good fit was obtained with χ_{aa} and $(1/\sqrt{6})(\chi_{bb} - \chi_{cc})$ as adjustable parameters and using an assumed set of rotational constants. However, it soon became apparent that the fit is independent of the rotational constants. Analytical expressions are available for $E(\kappa)$ and $E_Q(\kappa)$, the rotational and quadrupole interaction energies in terms of Ray's asymmetry parameter.[10] Inspection of them shows that E_Q is independent of κ for the $1_{10}, 1_{11}, 1_{01}$ and the $2_{21}, 2_{11}, 2_{12}$ levels, as are the allowed transitions among them (up to six R-branch transitions). However, E_Q for the 2_{20} and 2_{02} levels do depend on κ and so will transitions involving those levels. The expressions for E_Q are given only for a single quadrupolar nucleus, but we verified by numerical calculations that the overall dependence or nondependence on κ applies to two nuclei as well.
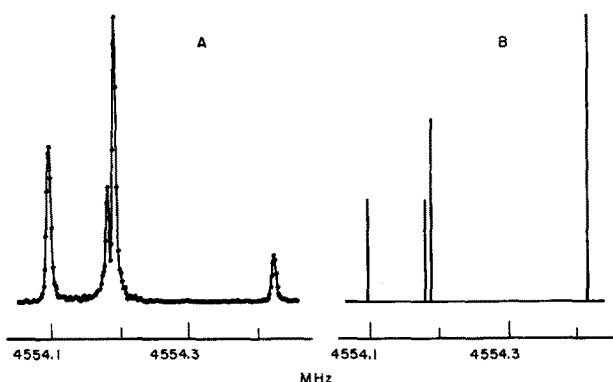
FIG. 2. High-resolution view (A) of the four low-frequency hf components of the $1_{11} \rightarrow 2_{12}$ transition in Fig. 1. The spectrum is an average of 4093 FIDs. The Doppler broadening is suppressed and the separation of the close doublet is 6 kHz. The fitted hfs is shown by the stick spectrum in B.

TABLE I. Observed and calculated hyperfine components for the $1_{11} \to 2_{12}$ and $1_{10} \to 2_{11}$ transitions of the ^{14}N, ^{14}N isotopic species of (HCN)$_2$–Ar.[a]

Component $F_1, F \to F_1', F'$	Observed (MHz)	Calculated (MHz)	Obs − calc (kHz)
	$1_{11} \to 2_{12}$		
1,1→1,1	4554.095	4554.097	− 2
1,0→1,1	4554.181	4554.183	− 2
0,1→2,2	4554.191	4554.189	2
2,2→2,3	4554.416	4554.415	1
2,3→2,3	4555.345	4555.344	1
1,2→1,3	4555.496	4555.495	1
2,2→2,1	4555.561	4555.564	− 3
0,1→2,1	4555.661	4555.657	4
1,1→1,1	4555.728	4555.730	− 2
2,2→0,2	4555.728	4555.730	− 2
0,1→0,2	4555.826	4555.823	3
1,2→1,2	4556.178	4556.179	− 1
2,3→2,4	4556.262	4556.261	1
1,1→1,2	4556.798	4556.797	1
2,1→2,1	4557.637	4557.639	− 2
2,1→0,2	4557.806	4557.805	1
2,1→2,0	4558.169	4558.170	− 1
	$1_{10} \to 2_{11}$		
2,2→2,2	6207.898	6207.896	2
1,0→1,1	6207.956	6207.957	− 1
0,1→2,2	6207.991	6207.993	− 2
2,2→2,3	6208.205	6208.204	1
2,3→2,3	6209.162	6209.166	− 4
1,2→1,3	6209.289	6209.290	− 1
2,2→0,2	6209.472	6209.473	− 1
1,1→1,1	6209.557	6209.559	− 2
0,2→0,1	6209.573	6209.570	3
1,2→1,2	6209.954	6209.951	3
2,3→2,4	6210.052	6210.051	1
1,1→1,2	6210.593	6210.591	2
2,1→2,1	6211.461	6211.461	0
2,1→0,2	6211.622	6211.622	0
2,1→2,0	6211.974	6211.975	− 1

[a] In the fit $\chi_{cc}(1)$ and $\chi_{cc}(2)$ were held constant at the values found for them in the mixed ^{14}N, ^{15}N species (see Table IV). Line centers obtained by fitting these and other transitions are given in Table III.

The values found for χ_{gg} of N(1) from the final fit of the 4556 MHz transition are − 4.054, 2.002, and 2.052 MHz for $g = a, b, c$, respectively (Table II). Those reported for N(1) of the free HC^{14}N–HC^{15}N dimer are − 4.106, 2.053, and 2.053 MHz.[1] The two sets of values are virtually identical. χ_{cc} is the same for both species, while χ_{aa} and χ_{bb} are slightly less for the cluster. This implies that the quadrupole interaction is the same (χ_s) as in the dimer but the a inertial axis of the cluster is rotated about the c axis by a few degrees (θ_{gs}) from the principal axis for the quadrupole interaction tensor. We can estimate the rotation angle by neglecting the torsion of the HCN monomers and taking the projection[10]

$$\chi_{gg}(\text{trimer}) = \chi_s(\text{dimer})(1/2)(3\cos^2\theta_{gs} - 1) \quad (2)$$

for $g = a,b$. In this manner, with the data from the ^{14}N,^{14}N trimer and dimer, (Table II) θ_{as} is found from χ_{aa} for N(1) to be 4.8°, while χ_{bb} gives the complement 85.0° for θ_{bs}. The results for N(2) give a slightly larger rotation of 6.9° for θ_{as} and a correspondingly smaller value (83.1°) for θ_{bs}. The results for the mixed ^{14}N/^{15}N trimers differ by a few degrees

TABLE II. Comparison of the hyperfine interaction constants for the HC ^{14}N subunits in the clusters with the results for the corresponding dimers.[a]

Isotopic species	^{14}N	(HCN)$_2$–Ar χ_{aa}	χ_{bb}	χ_{cc}	(HCN)$_2$[b] χ_{aa}
^{14}N,^{15}N	(1)	− 4.0335(14)	1.9819[c]	2.0516	− 4.1059(10)
^{15}N,^{14}N	(2)	− 4.3901(7)	2.1702[c]	2.2199(8)	− 4.4339(6)
^{14}N,^{14}N	(1)	− 4.054(24)	2.002	2.052[d]	− 4.097(20)
	(2)	− 4.334(22)	2.124	2.220[d]	− 4.440(19)

[a] The units are MHz and uncertainties are the standard deviation.
[b] From Ref. 1; $\chi_{bb} = \chi_{cc} = -(1/2)\chi_{aa}$.
[c] The fitted quantity is $(1/\sqrt{6})(\chi_{bb} - \chi_{cc})$; the standard deviation for it is given under χ_{cc}.
[d] These values for χ_{cc}, obtained for the mixed ^{14}N,^{15}N species, were held constant in fitting χ_{aa} as described in the text.

(Table III), attributable to rotation of the a,b-inertial axes by ^{15}N/^{14}N substitution.

Several conclusions can now be drawn. The cluster does contain the (HCN)$_2$ dimer as a subunit. The interactions between Ar and the (HCN)$_2$ dimer have at most a small effect upon the structure of the dimer. The (HCN)$_2$–Ar cluster is planar and its a axis is only about 6° from the axis of the linear (HC^{14}N)$_2$ subunit. Thus, the 4556 MHz transition is a dipole, which makes it either $1_{11} \to 2_{12}$ at $(B + 3C)$ or $1_{10} \to 2_{11}$ at $(3B + C)$. Moreover, in order for the a axis to nearly coincide with the (HCN)$_2$ axis, the cluster must be T shaped with the Ar on or close to the perpendicular bisector of a line joining the centers of mass (c.m.) for the two HCN's.

There was now sufficient information to estimate rotational constants. The value of B should be approximately that of the (HC^{14}N)$_2$ dimer, namely 1746 MHz. This requires that the 4556 MHz line be $1_{11} \to 2_{12}$ at $(B + 3C)$ rather than $1_{10} \to 2_{11}$ at $(3B + C)$, and leads to $C = 937$ MHz. Finally, the planarity condition gives A to be 2020 MHz.

A second group of lines was found at 4760 MHz, similar in breadth and complexity to that at 4556 MHz. Initial attempts to fit its hfs as the κ-dependent $1_{01} \to 2_{02}$ transition were unsuccessful even with the χ_{gg} values from the fit of the $1_{11} \to 2_{12}$ transition. Part of the problem is that the apparent intensities are readily distorted by their dependence on sev-

TABLE III. Angles between inertial and electric field gradient axes for ^{14}N in the (HCN)$_2$–Ar trimers.

Angle (deg)	(HC^{14}N)$_2$–Ar N(1)	N(2)	(HC^{14}N/HC^{15}N)–Ar N(1)	N(2)
	From χ_{gg}, torsional effects neglected			
θ_{as}	4.8	6.9	6.2	4.7
θ_{bs}	85.0	83.1	83.8	85.2
	From χ_{aa}, torsional effects included			
θ_{as}	5.7	6.7	6.6	4.6

eral different instrumental variables. This is evident in Fig. 2 for $1_{11} \rightarrow 2_{12}$ where the high-frequency component is much lower in relative intensity than predicted because it is farthest from the frequency to which the cavity was tuned. Also, the quadrupole interactions differ by less than 10% for the two ^{14}N's, making the fit and its κ dependence insensitive to their relative magnitudes.

Therefore, the search was turned to the two mixed ^{14}N/^{15}N isotopic species of the trimer, for which the hfs is much simpler. The rough rotational constants and molecular geometry were used to estimate frequencies for the ^{14}N/^{15}N counterparts of the 4556 and 4760 MHz transitions, the latter assumed to be $1_{01} \rightarrow 2_{02}$. They were soon found and the hfs fitted in the

$$J + I = F \tag{3}$$

basis for the single ^{14}N. The observed and fitted hfs is given in Table IV for several of the mixed species. Also, the analytical expression for the κ dependence of the hfs for the $1_{01} \rightarrow 2_{02}$ transition was used to find κ, 0.453 for the ^{14}N,^{15}N trimer and 0.531 for the ^{15}N,^{14}N. The two line-center frequencies were combined with κ to determine rigid rotor rotational constants and thereby locate other transitions. The final results for the line centers of the four isotopic species of the trimer are summarized in Table V.

More details of the hfs

The line centers were found for all observed transitions of the ^{14}N containing species by fitting of the hfs, only some of which is given in Tables I and IV. The quadrupole interaction constants obtained in the fitting are given in Table II; the earlier results for the four ^{14}N/^{15}N isotopic species of (HCN)$_2$ are included for comparison. It is seen that the two sets of values for the trimer match up with those in the free dimer, serving as a basis for assigning the positions of N(1) and N(2) in the trimer. The values for the two mixed ^{14}N/^{15}N trimers are more accurate than for the ^{14}N,^{14}N trimer, for the reasons mentioned above. In the case of (HC^{15}NHC^{14}N)–Ar the 21 components for 5 transitions (Table IV) were fitted simultaneously with no residue as large as a kHz. Thus, there is no measurable dependence of the χ's on J, at least for the low J's observed.

For the ^{14}N,^{14}N species fitting of the hfs by Eq. (1) to determine χ_{gg} was not nearly as accurate as the analysis for the single ^{14}N in the two mixed trimers. This was also the case for the (HCN)$_2$ dimer where the uncertainty in χ_{gg} from the homonuclear dimer is 20 to 30 times larger than that for the mixed species.[1] Therefore, in order to have good values of χ_{aa} for analyzing the orientation of the HC^{14}N monomers in the cluster, we fitted the hfs with χ_{cc} held constant for each ^{14}N at the value for it in the corresponding mixed cluster (Table II). This is justified because it has been shown that HC^{14}N/HC^{15}N substitution does not change appreciably the torsional averaging or charge redistribution effects on χ_{gg} in the dimer.[9] Also, to further improve the standard deviation of χ_{aa} the hfs was fitted simultaneously for both the $1_{11} \rightarrow 2_{12}$ and $1_{10} \rightarrow 2_{11}$ transitions. The results of this procedure are given in Tables I, IV, and V.

TABLE IV. Observed and calculated hyperfine components for several transitions of the ^{14}N,^{15}N mixed isotopic species of (HCN)$_2$–Ar.[a]

Component $F \rightarrow F'$	Observed (MHz)	Calculated (MHz)	Obs − calc (kHz)
(HC^{14}NHC^{15}N)–Ar $1_{11} \rightarrow 2_{12}$			
$1 \rightarrow 2$	4453.6311	4453.6316	− 0.5
$2 \rightarrow 2$	4454.2261	4454.2258	0.3
$1 \rightarrow 1$	4454.6578	4454.6579	− 0.1
$2 \rightarrow 3$	4454.8858	4454.8852	0.6
$0 \rightarrow 1$	4456.1435	4456.1439	− 0.4
(HC^{15}NHC^{14}N)–Ar $1_{11} \rightarrow 2_{12}$			
$1 \rightarrow 2$	4516.8501	4516.8502	− 0.1
$2 \rightarrow 2$	4517.5012	4517.5011	0.1
$2 \rightarrow 3$	4518.2145	4518.2146	− 0.1
$1 \rightarrow 1$	4519.5883	4519.5881	0.2
$1_{01} \rightarrow 2_{02}$			
$0 \rightarrow 1$	4718.3702	4718.3695	0.7
$1 \rightarrow 1$	4718.8383	4718.8388	− 0.5
$2 \rightarrow 3$	4719.8073	4719.8072	0.1
$1 \rightarrow 1$	4721.6618	4721.6621	− 0.3
$1_{10} \rightarrow 2_{11}$			
$1 \rightarrow 2$	6157.7790	6157.7797	− 0.7
$1 \rightarrow 1$	6158.8653	6158.8653	0.0
$2 \rightarrow 3$	6159.1437	6159.1428	0.9
$0 \rightarrow 1$	6160.5293	6160.5295	− 0.2
$2_{12} \rightarrow 3_{13}$			
$2 \rightarrow 3$	6463.7416	6463.7417	− 0.1
$1 \rightarrow 2$	6463.9784	6463.9790	− 0.6
$3 \rightarrow 4$	6464.0272	6464.0264	0.8
$2_{02} \rightarrow 3_{03}$			
$1 \rightarrow 2$	6506.6770	6506.6779	− 0.9
$2 \rightarrow 3$	6506.8040	6506.8033	0.7
$3 \rightarrow 4$	6506.8577	6506.8576	0.1

[a] The χ_{gg}'s and line centers obtained by fitting these and other transitions are given in Tables II and V.

TABLE V. Observed and fitted line centers[a] for rotational transitions of the four ^{14}N,^{15}N isotopic species of (HCN)$_2$–Ar.[b]

Transition $J_{K_pK_o} \rightarrow J'_{K_pK_o}$	14–14[c] (MHz)	14–15 (MHz)	15–14 (MHz)	15–15 (MHz)
$0_{00} \rightarrow 1_{01}$	2691.491	2623.234	2669.373	2603.568
$1_{11} \rightarrow 2_{12}$	4555.749	4454.639	4517.947	4419.638
$1_{01} \rightarrow 2_{02}$	4760.166	4683.514	4719.812	4643.532
$1_{10} \rightarrow 2_{11}$	6209.541	6037.665	6158.877	5994.004
$2_{12} \rightarrow 3_{13}$	6518.623	6395.932	6463.935	6343.280
$2_{02} \rightarrow 3_{03}$	6562.307	6454.960	6506.817	6399.857
$2_{21} \rightarrow 3_{22}$	8072.592	7867.990	8006.226	···
$2_{11} \rightarrow 3_{12}$	8597.626	8437.551	8525.197	8368.205
$2_{20} \rightarrow 3_{21}$	9584.487	9282.374	9507.303	9219.525
$3_{13} \rightarrow 3_{12}$	4559.698	···	···	···
$3_{03} \rightarrow 3_{22}$	4803.233	···	···	4706.925
$3_{22} \rightarrow 4_{23}$	10205.653	···	···	···
$4_{23} \rightarrow 4_{22}$	4268.655	···	···	···

[a] The calculated line centers differ from the observed for only four transitions, for which the difference is a kHz.
[b] The rotational constants obtained in the fitting are given in Table VI.
[c] The (HC^{i}NHC^{j}N)–Ar trimer is designated by $i - j$.

We now take a closer look at the relationship of the quadrupole interaction tensors for the ^{14}N's in the dimer to the inertial axes in the cluster. Equation (2) assumes the two to be rotated by static angles θ_{gs}. However, the experimental values found for θ_{as} and θ_{bs} are actually from the average of $(1/2)(3\cos^2\theta_{gs} - 1)$ over the zero-point torsional oscillations of the HCN in question. The projection is not linear in θ_{gs} so its value depends upon the torsional amplitude as well as on the rotation of the inertial axes. The two effects can be separated by the approximate deconvolution used for the H/DF dimers.[11,12] From Eq. (2) the observed hyperfine interaction constant is

$$\chi_{aa}(\text{obs}) = (\chi_s/2)\langle 3\cos^2\theta_{as} - 1\rangle_t, \qquad (4)$$

where the subscript t indicates an average over the torsion. The values for χ_s in the cluster are taken to be that of the HC^{14}N monomer, corrected for the charge redistribution effects in the dimer,[9] i.e., $\chi_s(1)$ and $\chi_s(2)$ are -4.4802 and -4.6029 MHz, respectively.

For a ground-state, planar harmonic torsional oscillator the expectation value in Eq. (4) is approximately

$$\langle\ \rangle_t = N \int_{-\pi}^{\pi} (3\cos^2\theta_{as} - 1)$$
$$\times \exp[\ -\beta^2(\theta_{as} - \theta_{as}^0)^2]d\theta_{as}, \qquad (5)$$

in which N is a normalizing constant, β is an inverse torsional amplitude, and θ_{as}^0 is the equilibrium value of θ_{as}, i.e., the "static" rotational angle between inertial and field gradient axes. Values were determined for β from the average torsional angles (13.6° and 9.0°) found for the HCN subunits in the dimer.[9] These angles were substituted on the left-hand side of Eq. (5) which was solved numerically for β with θ_{as}^0 set equal to zero; amplitudes of 19.3° and 12.85° were obtained. The rotational angle θ_{as}^0 was then found from χ_{aa}, χ_s, and β by combining Eqs. (4) and (5). The results are seen in Table III. Inclusion of the torsion in this manner changes θ_{as}^0 by less than a degree.

Rotational constants and substitution structure

The line centers of the a dipole transitions analyzed for the four ^{14}N/^{15}N isotopic species of the cluster are listed in

TABLE VI. Watson's determinable parameters obtained by using the Kirchhoff program with fourth-order centrifugal distortion to fit the line centers found for the four ^{14}N,^{15}N isotopic species of (HCN)$_2$–Ar.[a,b]

	14–14[c]	14–15	15–14	15–15
A''	2013.5993(10)	2005.7495	1995.8088	1985.6439
B''	1759.2756(3)	1707.4532	1744.9998	1695.4553
C''	932.3709(2)	915.9227	924.5311	908.2597
τ_1	$-0.3017(1)$	-0.2702	-0.3062	-0.2823
τ_2	$-0.0660(1)$	-0.0575	-0.0668	-0.0621
τ_{aaaa}	$-0.1700(9)$	-0.199	-0.164	-0.1604
τ_{bbbb}	$-0.01371(1)$	-0.0198	-0.0105	-0.0148
τ_{cccc}	$-0.0088(1)$	-0.0098	-0.0083	-0.0075
Δ	3.7881(2)	3.8211	3.7971	3.8306

[a] The inertial defect Δ is also given.
[b] The units are MHz except for Δ, which is in amu Å^2.
[c] The standard deviation is given here but not for the other species for which fewer line centers were fitted.

TABLE VII. Molecular constants derived for the four ^{14}N,^{15}N isotopic species of (HCN)$_2$–Ar from Watson's determinable parameters.[a]

	14–14	14–15	15–14	15–15
A	2013.531(2)	2005.690	1995.740	1985.578
B	1759.191(2)	1707.377	1744.915	1695.375
C	932.339(2)	915.892	924.498	908.232
τ_{aabb}	0.0071(37)	0.0202	0.0053	0.0080
τ_{abab}	$-0.1348(35)$	-0.1229	-0.1371	-0.1280

[a] The units are MHz. The uncertainties are the rms deviation of the three values averaged to obtain the results given here. See the text for details.

Table V. The transitions were fitted with the Hamiltonian of a distorted asymmetric rotor, using the computer program developed and described by Kirchhoff,[13] with centrifugal distortion constants (τ's) through fourth order and the rotational constants as adjustable parameters. The residues are a kHz or less, mainly less, so they are not given. The resulting values for Watson's determinable parameters[14] are listed in Table VI, also the inertial defect. Molecular constants derived from these parameters are given in Table VII. They include the τ-free rotational constants and values for τ_{aabb} and τ_{abab}. These properties may be derived using any two of τ_1, τ_2, and τ_{cccc}, with slightly different results. The values given are the average for the three sets of results. In our analysis of the structure we have used the effective moments of inertia corresponding to the τ-free rotational constants of Table VII. The conversion factor for $I \times B$ was 505 379.1 amu Å^2 MHz.

The determination of further details is complicated by the absence of symmetry in the cluster and by the relatively large inertial defect (3.8 amu Å^2). In spite of the latter the cluster does appear to be planar and our analysis has been simplified by assuming planarity. The rotational constants for the four ^{14}N/^{15}N isotopic clusters in Table VII enable the a,b coordinates of the two nitrogens to be located in the c.m. system of the parent cluster by the substitution method, using each cluster in turn as the parent.[10] The labeling of the nitrogens and the signs of their coordinates, as given in Fig. 3, are based unambiguously on the χ_{gg} and θ_{as} values listed in Tables II and III.
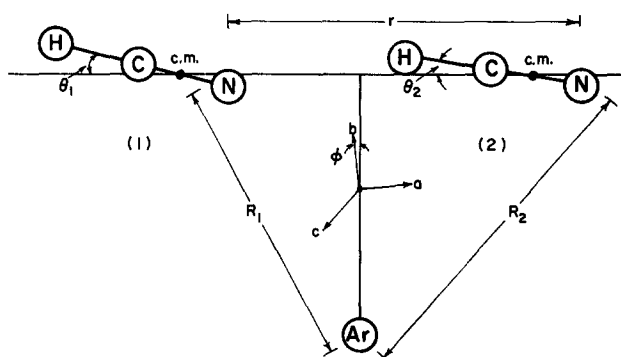

FIG. 3. Geometrical structure and coordinates used to describe (HCN)$_2$–Ar. The figure is to scale for the ^{14}N homodimer species. The origin of the inertial axes is placed at the c.m. for the cluster.

TABLE VIII. Structural parameters for the four ^{14}N,^{15}N isotopic species of (HCN)$_2$–Ar, determined from the rotational constants in Table VII.

Parameter	14–14	14–15	15–14	15–15
By the substitution method[a]				
r_s(Å)[b]	4.450	4.454	4.453	4.457
ϕ(deg)	5.72	9.86	2.17	6.89
R_1(Å)	3.675	3.671	3.672	3.668
R_2(Å)	4.320	4.316	4.317	4.312
From an inertial analysis[a]				
ϕ(deg)	4.97	9.34	1.83	6.40

[a] Average values obtained for the N$\cdots$N, Ar$\cdots$N(1), and Ar$\cdots$N(2) distances (r_s, R_1, R_2) by the substitution method are 4.453, 3.671, and 4.316 Å and from the inertial analysis 4.440, 3.658, and 4.358 Å.

[b] The r_s for (HCN)$_2$ dimer is 4.461 Å (Ref. 9).

A different choice of isotopic species as parent changes the a,b coordinates of the nitrogens, but it should have little effect on the N$\cdots$N distance (r_s). This is seen to be the case in Table VIII where the four values for r_s range from 4.450 to 4.457. Moreover, their average of 4.453 Å is quite close to the 4.461 Å r_s value found for the N$\cdots$N distance in the free dimer,[9] confirming that the weak forces between Ar and the (HCN)$_2$ dimer have at most a small effect on the structure of the dimer. In particular, it shows that the dimer is linear or very close to linear in the cluster. Taking this to be the case, the linear axis of the dimer goes through the substitution positions of the two nitrogens. Its slope in the a,b inertial frame gives the angle ϕ between the two axis systems, which is changed by isotopic substitution. The results for it are also listed in Table VIII.

The coordinates of Ar in the inertial frame of the parent cluster can be calculated from those of the two nitrogens by means of the c.m. conditions $\Sigma_i m_i a_i = 0$ and $\Sigma_i m_i b_i = 0$ for the cluster, treating it as pseudotriatomic. The a_i, b_i coordinates of each HCN are those of its c.m. They can be determined readily from those of the N by projecting the HCN's torsional oscillations onto the linear axis as was done for the (HCN)$_2$ dimer.[9] The c.m. of each HCN is on the linear axis. The substitution coordinates for the N correspond to projection onto that axis of the HCN at its average torsional angle θ. The c.m. of N(n) is the distance $r_N \cos \theta_n$ from N(n) along the axis, where r_N is the distance within the particular monomer between the N and the monomer's c.m. (Fig. 3). Values of 13.6° and 9° were used for θ_1 and θ_2, as found in our previous work on the dimer.

The argon coordinates determined in this manner combine with those for the nitrogens to give the two Ar$\cdots$N distances R_1 and R_2. The four values found for each are included in Table VIII. Their averages, 3.671 and 4.316 Å for R_1 and R_2, respectively, with that for r_s, lead to a perpendicular distance of 3.280 Å between the argon and the dimer axis. The perpendicular from the Ar (Fig. 3) is very close to the c.m. of the cluster, especially for the clusters with symmetrical (HCN)$_2$.

We explored analyzing the substitution data in Table VII as a nonplanar asymmetric top, using the expressions for the planar moments.[10] This has the possible advantage of obtaining a structure based on I_C as well as I_A and I_B. However, the approach gives small imaginary values ($<0.1i$ Å) for the c coordinates of the nitrogens and much the same results as presented above for a and b.

Inertial analysis

As a check on the substitution method we made several grid searches in which the four sets of inertial moments were fitted simultaneously, with the N$\cdots$N distance and the argon position as adjustable parameters. A linear, rigid, or equilibrium structure was usually assumed for the HCN dimer. A set of typical results is summarized in Table VIII. For this case the torsional oscillations were represented by two "half-mass" HCN's, each having the same c.m. as the corresponding free HCN and rotated by the average torsional angle from the linear axis for that position, but in opposite directions. The three distances found in this manner to give the smallest variance for the A and B rotational constants differ by about 0.02 Å from the substitution distances. The angle ϕ between the inertial and dimer axes is systematically somewhat larger ($\sim 0.5°$) than the substitution values for the four isotopic species.

A similar approach was used to explore effects of bending the two HCN's slightly (2°) from linearity in a rigid, linear N$\cdots$HCN arrangement. The fit of the rotational constants was improved by bending to give an umbrella shape. Bending in the opposite direction does not work at all. The slightly smaller value (1° to 2°) determined for θ_{as} of N(1) than for N(2) from χ_{gg} of (HC^{14}N)$_2$–Ar (Table III) corresponds to an umbrella bend. Therefore, it seems possible that cluster formation does cause the outer ends of the (HCN)$_2$ dimer to bend in very slightly toward the argon. In this bent (2°) version, the ϕ's calculated for HCN(2) are close to those determined for a linear dimer from the rotational constants (Table VIII).

DISCUSSION

The structure of the cluster reflects the two types of interaction within it. First, there is the hydrogen bonding which forms the linear (HCN)$_2$ dimer. It is localized, quite directional, and relatively strong (~ 1500 cm^{-1}).[1,2] Then there is the weak attraction between the argon and the π electrons of the two –C$\equiv$N groups. It is optimized by location of the argon alongside the dimer, equidistant from the centers of the two C$\equiv$N groups. The argon to dimer axis distance of 3.28 Å is exceptionally short compared with the 3.54 $\pm$ 0.07 range previously found for a number of T-shaped complexes between argon and π-electron polyatomics such as (CN)$_2$[15] and ClCN.[16] The difference may reflect the small, effective van der Waals radius of the N$\cdots$H–C hydrogen bond in the dimer.

Perturbation of the (HCN)$_2$ structure by its interaction with the argon is probably present but small. The electric field gradients at ^{14}N are not affected visibly. However, the slightly shorter N$\cdots$N r_s distance, 4.453 Å in the cluster vs 4.461 Å in the dimer, could be contraction mediated by the argon. Evidence for an umbrella-like bending of the dimer in the cluster is suggestive at best, but it would be a plausible effect of the argon.

The orientation of the dimer with respect to the inertial axes of the cluster was approached in two ways—from projection of the ^{14}N quadrupole interaction on the **a** axis (Table III) and from analysis of the rotational constants (Table VIII). In the latter, rotation of the inertial axes with respect to the dimer axis is very sensitive[16] to location of the argon. For (HC^{14}N)$_2$–Ar the results for the two methods are in excellent agreement. χ_{aa}, including torsional effects, gives θ_{as} to be 5.7° for N(1) and 6.7° for N(2). The substitution method gives $\phi = 5.7°$. The results for the mixed ^{14}N/^{15}N clusters are less consistent. θ_{as} is 6.6° for the ^{14}N,^{15}N cluster and 4.6° for the ^{15}N,^{14}N while the ϕ's are 9.9° and 2.2°. The differences indicate the limitations of the structural model employed.

A more sophisticated analysis would include the force field and normal coordinates, as was done for the ArClCN dimer.[16] However, the (HCN)$_2$ dimer cannot be treated as rigid nor is its force field known. So there are seven intermolecular modes to be determined in the cluster and only four independent τ's measured, a situation discouraging this approach.

Dykstra has recently developed methods for the efficient calculation in weakly bonded clusters of electrically based intermolecular potentials which include full mutual polarization effects.[17] Application of them to the Ar/HCN system appears to be an interesting test of their utility, with details forthcoming.[18] Some preliminary results relevant to the present account are as follows. The T-shaped structure reported here is predicted to be a local minimum in the potential surface for the (HCN)$_2$/Ar system, with an interaction energy of 1940 cm^{-1}. By way of comparison, the interaction energies at the same level of treatment for the linear Ar–HCN and (HCN)$_2$ dimers are 200 and 1830 cm^{-1}, respectively. Both linear forms of the trimer, Ar–HCNHCN and HCNHCN–Ar, are also at potential minima, of 2070 and 1990 cm^{-1}, respectively. Searches for them are planned.

ACKNOWLEDGMENTS

[1] L. W. Buxton, E. J. Campbell, and W. H. Flygare, Chem. Phys. **56**, 399 (1981).

[2] K. Georgiou, A. C. Legon, D. J. Millen, and P. J. Mjöberg, Proc. R. Soc. London Ser. A **399**, 377 (1985).

[3] R. S. Ruoff, T. Emilsson, T. D. Klots, C. Chuang, and H. S. Gutowsky, 41st Symposium on Molecular Spectroscopy, Columbus, OH, 1986, Abstract TF13.

[4] R. S. Ruoff, T. D. Klots, C. Chuang, T. Emilsson, and H. S. Gutowsky, 42nd Symposium on Molecular Spectroscopy, Columbus, OH, 1987, Abstract MG14.

[5] K. R. Leopold, G. T. Fraser, F. J. Lin, D. D. Nelson, and W. Klemperer, J. Chem. Phys. **81**, 4922 (1984).

[6] T. D. Klots, R. S. Ruoff, C. Chuang, T. Emilsson, and H. S. Gutowsky (to be published).

[7] E. J. Campbell, W. G. Read, and J. A. Shea, Chem. Phys. Lett. **94**, 69 (1983). The Mark I version is described in detail in several papers the last of which is T. J. Balle and W. H. Flygare, Rev. Sci. Instrum. **52**, 33 (1981).

[8] A series of modifications has been made in the spectrometer. See, for example, T. D. Klots, C. Chuang, R. S. Ruoff, T. Emilsson, and H. S. Gutowsky, J. Chem. Phys. **86**, 5315 (1987), and references cited therein.

[9] R. S. Ruoff, T. Emilsson, C. Chuang, T. D. Klots, and H. S. Gutowsky, Chem. Phys. Lett. **138**, 553 (1987).

[10] W. Gordy and R. L. Cook, *Microwave Molecular Spectra* (Wiley, New York, 1984).

[11] B. J. Howard, T. R. Dyke, and W. Klemperer, J. Chem. Phys. **81**, 5147 (1984).

[12] H. S. Gutowsky, C. Chuang, J. D. Keen, T. D. Klots, and T. Emilsson, J. Chem. Phys. **83**, 2070 (1985).

[13] W. H. Kirchhoff, J. Mol. Spectrosc. **41**, 1333 (1972).

[14] J. K. G. Watson, J. Chem. Phys. **46**, 1935 (1967).

[15] W. L. Ebenstein and J. S. Muenter, J. Chem. Phys. **80**, 1417 (1984).

[16] M. R. Keenan, D. B. Wozniak, and W. H. Flygare, J. Chem. Phys. **75**, 631 (1981).

[17] C. E. Dykstra, J. Phys. Chem. **91**, 6216 (1987); J. Comput. Chem. (submitted).

[18] C. E. Dykstra and H. S. Gutowsky (to be published).